
CompNet: Neural networks growing via the compact network morphism

Jun Lu*, Wei Ma*, Boi Faltings

Swiss Federal Institute of Technology (EPFL), Lausanne, Switzerland
junlulocky@gmail.com, ma.wei@epfl.ch, boi.faltings@epfl.ch

Abstract

It is often the case that the performance of a neural network can be improved by adding layers. In real-world practices, we always train dozens of neural network architectures in parallel which is a wasteful process. We explored *CompNet*, in which case we morph a well-trained neural network to a deeper one where network function can be preserved and the added layer is compact. The work of the paper makes two contributions: a). The modified network can converge fast and keep the same functionality so that we do not need to train from scratch again; b). The layer size of the added layer in the neural network is controlled by removing the redundant parameters with sparse optimization. This differs from previous network morphism approaches which tend to add more neurons or channels beyond the actual requirements and result in redundancy of the model. The method is illustrated using several neural network structures on different data sets including MNIST and CIFAR10.

1 Introduction

Over the recent decades, deep learning and neural networks have been used in a wide range of applications, e.g. computer vision [7, 16, 24, 25], natural language processing [1, 6, 14], financial forecasting and time series [8, 15, 19]. All of these applications need to train the neural networks in several days or even more than a month. If it turns out that we need to modify the neural network structure, it is either an immense waste of computational resources, or extremely prolonged experimentation cycles to train from scratch again. This kind of modification to the well trained neural network structure can usually happen in tasks where the amount of data increases, where we may always try to add additional layers to the old structure.

In the meanwhile, deep learning requires huge computing resources and memory. In practice, a device designed for training the network may not have enough resource or time to train a complex neural network, e.g., mobile devices usually have small storage and limited computing ability. We also often make modifications to the neural network according to the training and validation performance and then retrain the new model. The process is time consuming and wasteful. Our work accelerates retrain the process and makes the new network model keep the same function as the previous one.

In order to accelerate the training and exploration of deep neural network structure, there has been already some works on making a new network inherit the knowledge of the parent model for the same task. Net2Net [4] proposes a method based on the concept of function-preserving transformation. But Net2Net can only add a layer with specific neuron size. Network morphism (NetMorph) [28] approaches the inheritance problem by deconvolutional operation and actually there is no criteria to select the neuron size and it always makes the network structure much larger than expected. Specifically speaking, Net2Net and NetMorph only consider increasing the size of the neural network but not limiting the growth of complexity.

*Equal contribution.

On the other hand, researchers tend to modify the neural network structure empirically. Although there are some works on constructing the neural network automatically, e.g., Google [2, 23] has been exploring ways to automate the design of machine learning models and [3] proposes an approach for automatic construction of binary classifier of Recurrent Neural Network (RNN). However, most of the researchers look for a good architecture manually and empirically. In the paper, we propose a framework to speed up and control the process of increasing the model size.

Our method is illustrated on multilayer perceptron (MLP) and convolutional network. [20] shows that a convolutional layer can be transformed to a dense layer, which does not affect the learning process. Based on the conclusion, the traditional methods that work over matrix multiplication can be applied to the convolutional layers easily.

Recently, some compression methods are used to reduce the model size in deep learning. [5] investigates into the methods of compression of neural network and summarizes four types of methods: a). Parameter pruning and sharing. b). Low-rank factorization. c). Transfer/compact convolutional filters. d). Knowledge distillation [13]. For feature selection, [21] compares Lasso, Ordinary Least Square and ridge regression and finds that Lasso can work better than the others. [12] uses Lasso to accelerate very deep convolutional neural networks. [27] points out that the traditional Lasso tends to keep the relevant features and some independent but important features sometimes are removed. They solve the problem by penalizing the similarity matrix of the features. In our framework, we adopt this variant of Lasso.

Notation: In the paper, scalar variables are written as non-bold font lowercases, e.g., c and s are scalar values. Matrices and vectors are written as bold font capitals or bold font lowercases. For example, $\mathbf{W} \in \mathbb{R}^{a \times b}$ represents a matrix of size $a \times b$. We use \mathbf{W}_i to denote the i^{th} column of matrix \mathbf{W} , $\mathbf{W}_{j,:}$ to denote the j^{th} row of matrix \mathbf{W} . We use the superscripts to indicate the layer index of the neural network, e.g. $L^{(1)}$ is the first layer of the structure.

2 Proposed Method

When operating in a continuous learning setting such as reinforcement learning, we tend to use deeper neural networks to get better result without overfitting as we collect more data. And training the new neural network from scratch can be extremely time consuming. In this section, we describe our proposed algorithms. Briefly speaking, our methods take two steps. In the first step, we generate the child model by adding an additional layer and make it inherit the ability from the parent model by regression algorithms. In the second step, we use sparse optimization methods (e.g. Lasso) to reduce the size of the new layers. To illustrate, we use multilayer perceptron (MLP) as an example as shown Figure 1. But our work can be extended to convolutional neural networks (CNN) easily from the equivalence between fully connected layers and convolutional layers [9, 20].

2.1 Problem and Notation

Consider the fully connected layer structure shown in Figure 1. Figure 1a is a part of a well-tuned parent network and it represents two-layer structure of the parent network. Figure 1b is a child network after inserting a fully connected layer into the part of Figure 1a. We denote the output of layer $L^{(1)}$ and $L^{(2)}$ in Figure 1a by $\mathbf{O}^{(1)'}$ and $\mathbf{O}^{(2)'}$ respectively. And we denote the activation output of layer $L^{(1)}$ and $L^{(2)}$ in Figure 1a by $\mathbf{A}^{(1)'}$ and $\mathbf{A}^{(2)'}$ respectively. Note here that we use a prime to indicate whether it is the output or activation output of each layer in the original setting or not. In Figure 1b, we denote the output of layers $L^{(1)}$, $L^{(new)}$ and $L^{(2)}$ to be $\mathbf{O}^{(1)}$, $\mathbf{O}^{(new)}$ and $\mathbf{O}^{(2)}$ respectively. $\mathbf{A}^{(1)}$, $\mathbf{A}^{(new)}$ and $\mathbf{A}^{(2)}$ are the activation output of the corresponding layers. The activation function is denoted by $h(x)$, i.e. $\mathbf{A}^d = h(\mathbf{O}^d)$, $\forall d \in \{(1), (2), (new), (1)', (2)'\}$.

As stated, we have two targets: a). let the child network inherit the competence and preserve the functionality of the parent network. Thus after morphing, we want $\mathbf{A}^{(2)}$ to be as close to $\mathbf{A}^{(2)'}$ as possible, thus $\mathbf{O}^{(2)}$ is as close to $\mathbf{O}^{(2)'}$ as possible; b). sparsify the new layer to control the increase of complexity and reduce correlated neurons, i.e. we want the size of layer $L^{(new)}$ to be compact.

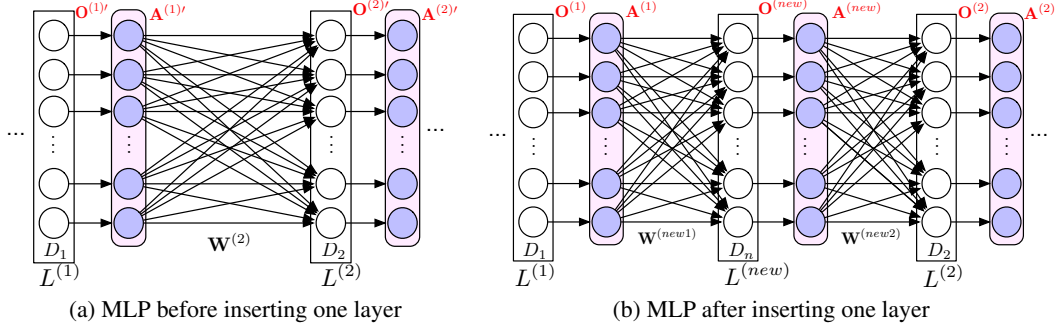


Figure 1: **Notations for our approach.** Figure 1a is a part of the parent network and Figure 1b is a child network after inserting a new layer into the part of Figure 1a. D_d is the number of the neurons in the layers and $L^{(d)}$ is the layer name, where $d \in \{1, 2, n\}$. $\mathbf{W}^{(2)}$ and $\mathbf{W}^{(new2)}$ are the weights of $L^{(2)}$ in Figure 1a and Figure 1b respectively. $\mathbf{W}^{(new1)}$ is the weights of the new layer $L^{(new)}$. The shallow pink box is the activation function layer. Note here $\mathbf{O}^{(1)} = \mathbf{O}^{(1)'}$ and $\mathbf{A}^{(1)} = \mathbf{A}^{(1)'}$.

2.2 Algorithm

We propose three algorithms to add an additional layer into the well trained neural network compactly. Algorithm 1 and 2 reduce the neuron size of $L^{(new)}$ directly by applying the sparse optimization to $\mathbf{W}^{(new1)}$. And Algorithm 3 reduces the neuron size of $L^{(new)}$ by applying the sparse optimization to $\mathbf{W}^{(new2)}$.

2.2.1 Reduce the neuron size of $L^{(new)}$ from $\mathbf{W}^{(new1)}$

Consider the problem shown in Section 2.1 and using the notation from Figure 1. In the article, when considering the optimization in layer $L^{(new)}$, we have $\mathbf{A}^{(1)} \in \mathbb{R}^{N \times D_1}$ as the input variable and $\mathbf{O}^{(new)} \in \mathbb{R}^{N \times D_n}$ as the response variable, $\mathbf{W}^{(new1)} \in \mathbb{R}^{D_1 \times D_n}$ as the weight matrix of layer $L^{(new)}$. When considering the optimization in layer $L^{(2)}$, we have $\mathbf{A}^{(new)} \in \mathbb{R}^{N \times D_n}$ as the input variable and $\mathbf{O}^{(2)' } \in \mathbb{R}^{N \times D_2}$ as the response variable.

Algorithm 1: In Algorithm 1, we firstly initialize $\mathbf{W}^{(new1)}$ according to the activation function (i.e. we have different initialization methods for different activation functions, e.g. TanH, Sigmoid or ReLU functions) [10, 17]. And then we get $\mathbf{O}^{(new)}$ by forward propagation from layer $L^{(new)}$ with the initialized weight $\mathbf{W}^{(new1)}$, i.e. $\mathbf{O}^{(new)} = \mathbf{A}^{(1)} \times \mathbf{W}^{(new1)}$. Afterwards we sparsify the neurons in $\mathbf{W}^{(new1)}$ by Lasso-related algorithms through minimizing Eq (1),

$$loss_1^{(alg1)} = \frac{1}{2N} \sum_{i=1}^{D_n} \left\| \mathbf{O}_i^{(new)} - \beta_i \mathbf{A}^{(1)} \mathbf{W}_i^{(new1)} \right\|_2^2 + \lambda (\|\beta\|_1 + \frac{\alpha}{2} |\beta|^\top \mathbf{R} |\beta|), \quad (1)$$

where the similarity matrix \mathbf{R} is defined by Eq (7). We can note that $\sum_{i=1}^{D_n} \|\mathbf{O}_i^{(new)} - \mathbf{A}^{(1)} (\beta_i \mathbf{W}_i^{(new1)})\|_2^2$ in Eq (1) is equal to $\|\mathbf{O}^{(new)} - \mathbf{A}^{(1)} (\mathbf{W}^{(new1)} \cdot \text{diag}(\beta))\|_F^2$, where $\text{diag}(\cdot)$ operator maps a vector to a diagonal matrix whose diagonal is the elements of the vector. More detailed analysis of this sparse optimization is delayed to Section 2.3.

Finally, we optimize $\mathbf{W}^{(new2)}$ via least squares:

$$loss_2^{(alg1)} = \frac{1}{2N} \left\| \mathbf{O}^{(2)' } - \mathbf{A}^{(new)} \mathbf{W}^{(new2)} \right\|_F^2 = \frac{1}{2N} \left\| \text{vec}(\mathbf{O}^{(2)' }) - \text{vec}(\mathbf{A}^{(new)} \mathbf{W}^{(new2)}) \right\|_2^2, \quad (2)$$

where $\text{vec}(\cdot)$ is the vectorization operator. Here we can also use ridge regression to penalize the scale of $\mathbf{W}^{(new2)}$. Note here that we use $\mathbf{O}^{(2)' }$ as the target response because we want our output $\mathbf{O}^{(2)} = \mathbf{A}^{(new)} \mathbf{W}^{(new2)}$ to be as close to the original output $\mathbf{O}^{(2)' }$ as possible.

Algorithm 2: In Algorithm 1, we only optimize β by minimizing $loss_1^{(alg1)}$. The other choice is that we optimize β and $\mathbf{W}^{(new1)}$ by minimizing $loss_1^{(alg2)}$ alternatively as shown in Algorithm 2. The superscripts of $loss_1^{(alg2)}$ and $loss_1^{(alg1)}$, $loss_2^{(alg2)}$ and $loss_2^{(alg1)}$ are used to distinguish different algorithms but they are exactly the same in Algorithm 1 and 2. For optimizing $\mathbf{W}^{(new2)}$, Algorithm 2 takes the same operation as Algorithm 1. The motivation of the second algorithm is to reconstruct the output after sparsifying.

2.2.2 Reduce the neuron size of $L^{(new)}$ from $\mathbf{W}^{(new2)}$

Algorithm 3: To reduce the size of $L^{(new)}$ and its corresponding weight matrix $\mathbf{W}^{(new1)}$, another choice is to make $\mathbf{W}^{(new1)}$ of size $D_1 \times D_n$ smaller by reducing $\mathbf{W}^{(new2)}$ of size $D_n \times D_2$ as shown by Algorithm 3 because $\mathbf{W}^{(new2)}$ shares the first dimension with the feature dimension of $\mathbf{W}^{(new1)}$ which is D_n .

In this algorithm, we firstly initialize $\mathbf{W}^{(new1)}$ according to the activation function same as Algorithm 1. Then we forward propagate to get $\mathbf{A}^{(new)} = h(\mathbf{A}^{(1)} \times \mathbf{W}^{(new1)})$. Afterwards, we initialize $\mathbf{W}^{(new2)}$ via least squares as shown in Eq (2) but we denote Eq (2) as $loss_2^{(alg3)}$ to differentiate the algorithms. Finally, we sparsify the neurons in layer $L^{(new)}$ by:

$$loss_1^{(alg3)} = \frac{1}{2N} \left\| \mathbf{O}^{(2)'} - \sum_{i=1}^{D_n} \beta_i \mathbf{A}_i^{(new)} \mathbf{W}_{i,:}^{(new2)} \right\|_F^2 + \lambda (\|\beta\|_1 + \frac{\alpha}{2} |\beta|^\top \mathbf{R} |\beta|), \quad (3)$$

where $\mathbf{O}^{(2)'}$ is the original output of Layer $L^{(2)}$ as shown in Figure 1a.

However, Algorithm 3 has much higher complexity compared with Algorithm 1 and 2 due to the sum operation $\sum_{i=1}^{D_n} \beta_i \mathbf{A}_i^{(new)} \mathbf{W}_{i,:}^{(new2)}$. And this process takes a longer time to compute than Algorithm 1 and 2. Especially, when applying Algorithm 3 to convolutional layer, the cost time is scaled by the number of channels and the size of matrix is usually very large so that the speed is very slow and sometimes memory error happens. To accelerate the Algorithm 3, we can sample on the intermediate output (rows of $\mathbf{A}_i^{(new)}$) of the layers according to [12].

An important computational property for Eq (3) is that the first term can be rewritten as:

$$\frac{1}{2N} \left\| vec(\mathbf{O}^{(2)'}) - [vec(\mathbf{T}_1), vec(\mathbf{T}_2), \dots, vec(\mathbf{T}_{D_n})] \beta \right\|_2^2, \quad (4)$$

where $\mathbf{T}_i = \mathbf{A}_i^{(new)} \mathbf{W}_{i,:}^{(new2)}$, $\forall i \in \{1, 2, \dots, D_n\}$ and $vec(\cdot)$ is the vectorization operator.

2.3 Sparsify the neurons in the newly added layer

2.3.1 Interpretation of Lasso in our algorithms

Consider the sparse optimization in Algorithm 1 and 2, let $\beta = (\beta_1, \beta_2, \dots, \beta_i, \dots, \beta_{D_n})^\top$, Lasso optimization for β in our problem is defined by

$$\beta = \underset{\beta}{\operatorname{argmin}} \frac{1}{2N} \left\| \mathbf{O}^{(new)} - \mathbf{A}^{(1)} \mathbf{W}^{(new1)} \cdot \operatorname{diag}(\beta) \right\|_F^2 + \lambda \|\beta\|_1, \text{ where } \mathbf{O}^{(new)} = \mathbf{A}^{(1)} \mathbf{W}^{(new1)}. \quad (5)$$

Lasso can give the solution with some exact zeros. So when β_i is zero, the corresponding feature $\mathbf{W}_i^{(new1)}$ will be removed.

In our method, β_j should be in the range of $[0, 1]$ to indicate the importance of each neuron. But in our proposal, we initialized $\mathbf{O}^{(new)}$ by $\mathbf{O}^{(new)} = \mathbf{A}^{(1)} \cdot \mathbf{W}^{(new1)}$. We can easily find that each β_i cannot be negative value when the algorithm converges, because it will cause larger loss in both first term and second term of Eq (5) when $\beta_i < 0$ than $\beta_i = 0$; and also each β_i cannot be larger than 1 because it will cause loss in first term of Eq (5) and impose larger loss in second term of Eq (5) than the loss of the second term when each $\beta_i = 1$. So this constraint can be relaxed.

2.3.2 Independently interpretable Lasso

In our work, we use a modification of Lasso algorithm which is called independently interpretable Lasso (iiLasso) [27] that can suppress selecting correlated variables by penalizing the similarity of

the predictable variables. In our problem iiLasso is defined by Eq (6),

$$\boldsymbol{\beta} = \underset{\boldsymbol{\beta}}{\operatorname{argmin}} \frac{1}{2N} \|\mathbf{O}^{(new)} - \mathbf{X} \cdot \mathbf{B}\|_F^2 + \lambda(\|\boldsymbol{\beta}\|_1 + \frac{\alpha}{2} |\boldsymbol{\beta}|^\top \mathbf{R} |\boldsymbol{\beta}|), \quad (6)$$

where $\mathbf{X} = \mathbf{O}^{(new)} = \mathbf{A}^{(1)} \mathbf{W}^{(new1)} \in \mathbb{R}^{N \times D_n}$, $\mathbf{B} = \operatorname{diag}(\boldsymbol{\beta})$ and $\mathbf{R} \in \mathbb{R}^{D_n \times D_n}$ is a symmetric matrix whose component $\mathbf{R}_{jk} \geq 0$ represents the similarity between \mathbf{X}_j and \mathbf{X}_k and its component is defined by Eq (7):

$$\text{standardize } \mathbf{O}_i^{(new)}, \text{ and } \mathbf{X}_i, \forall i \in \{1, 2, \dots, D_n\}$$

$$\mathbf{r}_{jk} = \frac{1}{N} |\mathbf{X}_j^\top \mathbf{X}_k|, \quad \mathbf{R}_{jk} = \begin{cases} \frac{|\mathbf{r}_{jk}|}{1 - |\mathbf{r}_{jk}|} & j \neq k, \\ 0 & j = k. \end{cases} \quad (7)$$

The last term of the Eq (6) can also be written as $\frac{\lambda\alpha}{2} \sum_{j=1}^{D_n} \sum_{k=1}^{D_n} \mathbf{R}_{jk} |\beta_j| |\beta_k|$. In this case, if the correlation between two certain neuron variables becomes higher, i.e. $\mathbf{r}_{jk} \rightarrow 1$, we penalize larger for the two neurons. When \mathbf{R}_{jk} goes infinity, we can set either β_j or β_k to be zero. We can easily interpret that when two inputs \mathbf{X}_j and \mathbf{X}_k are highly similar, we will impose larger loss in the last term of Eq (6) so that we will enforce either β_j or β_k to be closer to zero. And notice that $\mathbf{X} = \mathbf{A}^{(1)} \mathbf{W}^{(new1)}$ so that the penalization of two neurons for the similarity is decide both by activation output $\mathbf{A}^{(1)}$ and weight matrix $\mathbf{W}^{(new1)}$. And because all the components in the last term of Eq (6) is not negative, i.e. $|\beta_j| \geq 0$, $\mathbf{R}_{jk} \geq 0$, we can still relax the constraint that $\beta_j \in [0, 1]$. And this algorithm can easily be extended to Algorithm 3 from Eq (3).

Algorithm 1: Sparsify $\mathbf{W}^{(new1)}$, optimize $\mathbf{W}^{(new2)}$	Algorithm 2: Alternatively update
<pre> begin Step 1: Initialize $\mathbf{W}^{(new1)}$ accordingly and initialize $\boldsymbol{\beta}$ to ones vector; Step 2: Compute $\mathbf{O}^{(2)'}$, $\mathbf{A}^{(1)}$, $\mathbf{O}^{(new)}$ and $\mathbf{X} = \mathbf{A}^{(1)} \mathbf{W}^{(new1)}$; Step 3: Standardize $\mathbf{O}^{(new)'}$ and \mathbf{X} so that column vector: $\operatorname{mean}(\mathbf{O}_i^{(2)'}) = 0$, $\operatorname{mean}(\mathbf{X}_i) = 0$ and $\mathbf{X}_i^\top \mathbf{X}_i = N$; Step 4: Compute similarity matrix \mathbf{R} of \mathbf{X}; Step 5: while $i < \max_itr$ or $\ \boldsymbol{\beta}\ _0 < c$ do $\boldsymbol{\beta} = \underset{\boldsymbol{\beta}}{\operatorname{argmin}} \operatorname{loss}_1^{(alg1)}$; end Step 6: Drop the column i of $\mathbf{W}^{(new1)}$ if β_i is zero; Step 7: Compute $\mathbf{A}^{(new)} = h(\mathbf{A}^{(1)} \mathbf{W}^{(new1)})$; Step 8: $\mathbf{W}^{(new2)} = \underset{\mathbf{W}^{(new2)}}{\operatorname{argmin}} \operatorname{loss}_2^{(alg1)}$; return $\mathbf{W}^{(new1)}$ and $\mathbf{W}^{(new2)}$. end </pre>	<pre> begin Step 1, 2, 3, 4 same as Algorithm 1; Step 5: while $i < \max_itr$ or $\ \boldsymbol{\beta}\ _0 < c$ do Step 5.1: Fix $\mathbf{W}^{(new1)}$, optimize $\boldsymbol{\beta} = \underset{\boldsymbol{\beta}}{\operatorname{argmin}} \operatorname{loss}_1^{(alg2)}$; Step 5.2: Fix $\boldsymbol{\beta}$, optimize $\mathbf{W}^{(new1)} = \underset{\mathbf{W}^{(new1)}}{\operatorname{argmin}} \operatorname{loss}_1^{(alg2)}$; end Step 6, 7, 8 same as Algorithm 1; return $\mathbf{W}^{(new1)}$ and $\mathbf{W}^{(new2)}$. end </pre>

Algorithm 3: Reduce $\mathbf{W}^{(new1)}$ by optimizing $\mathbf{W}^{(new2)}$
<pre> begin Step 1: Initialize $\mathbf{W}^{(new1)}$ according to the activation function and initialize $\boldsymbol{\beta}$ to ones vector; Step 2: Compute $\mathbf{O}^{(2)'}$, $\mathbf{A}^{(1)}$, $\mathbf{A}^{(new)}$ and \mathbf{T}_i, where $\mathbf{T}_i = \mathbf{A}_i^{(new)} \mathbf{W}_{i,:}^{(new2)}, \forall i \in \{1, 2, \dots, D_n\}$; Step 3: $\mathbf{W}^{(new2)} = \underset{\mathbf{W}^{(new2)}}{\operatorname{argmin}} \operatorname{loss}_2^{(alg3)}$; Step 4: Standardize $\operatorname{vec}(\mathbf{O}^{(2)'})$ and $\operatorname{vec}(\mathbf{T}_i)$ so that $\operatorname{mean}(\operatorname{vec}(\mathbf{O}^{(2)'})) = 0$ and $\operatorname{mean}(\operatorname{vec}(\mathbf{T}_i)^\top \operatorname{vec}(\mathbf{T}_i)) = 1$; Step 5: Compute similarity matrix \mathbf{R} from \mathbf{T}_i; Step 6: while $i < \max_itr$ or $\ \boldsymbol{\beta}\ _0 < c$ do $\boldsymbol{\beta} = \underset{\boldsymbol{\beta}}{\operatorname{argmin}} \operatorname{loss}_1^{(alg3)}$; end Step 7: Drop column i of $\mathbf{W}^{(new1)}$ and row i of $\mathbf{W}^{(new2)}$ if β_i is zero; return $\mathbf{W}^{(new1)}$ and $\mathbf{W}^{(new2)}$. end </pre>

2.4 Optimization solution for β

β is a vector whose every component corresponds to one feature. We use coordinate descent to tackle this optimization problem. And when $\beta_j = 0$, we drop the corresponding feature (i.e. neuron in neural networks). Lemma 2.1 gives the closed form solution for the update of each coordinate β_j in Algorithm 1, 2 and 3.

Lemma 2.1. *For the iiLasso problem in Algorithm 1 and 2, we can get the best value for each coordinate by closed form:*

$$\beta_j = \frac{1}{1 + \alpha \lambda \mathbf{R}_{jj}} S \left(\frac{1}{N} \mathbf{O}_j^{(new)\top} \mathbf{X}_j, \lambda(1 + \alpha \sum_{c=1, c \neq j}^{D_n} \mathbf{R}_{jc} |\beta_c|) \right), \quad (8)$$

And for Algorithm 3, the solution is :

$$\beta_j = \frac{1}{1 + \alpha \lambda \mathbf{R}_{jj}} S \left(\frac{1}{N \times D_2} [\text{vec}(\mathbf{O}^{(2)'}) - \sum_{i=1, i \neq j}^{D_n} \beta_i \cdot \text{vec}(\mathbf{T}_i)]^\top \mathbf{T}_j, \lambda(1 + \alpha \sum_{c=1, c \neq j}^{D_n} \mathbf{R}_{jc} |\beta_c|) \right), \quad (9)$$

where

$$S(a, b) = \text{sgn}(a)(|a| - b)_+ = \begin{cases} a - b, & a > 0 \text{ and } b < |a|, \\ a + b, & a < 0 \text{ and } b < |a|, \\ 0, & |a| < b. \end{cases} \quad (10)$$

2.5 Optimization solution for $\mathbf{W}^{(new1)}$

In the Algorithm 2, for $\min \text{loss}_1^{(alg2)}$, we can get the solution directly by $\frac{\partial \text{loss}_1^{(alg2)}}{\partial \mathbf{W}^{(new1)}} = 0$. And we get $\mathbf{W}^{(new1)} = (\mathbf{C}^\top \mathbf{C})^{-1} \mathbf{C}^\top \mathbf{O}^{(new)}$, where $\mathbf{C} = \mathbf{A}^{(1)} \cdot \text{diag}(\beta)$.

2.6 Optimization solution for $\mathbf{W}^{(new2)}$

The optimization of $\mathbf{W}^{(new2)}$ for $\text{loss}_2^{(alg1)}$ and $\text{loss}_2^{(alg2)}$ in Algorithm 1 and 2 is a problem of least squares. We take the gradient of $\text{loss}_2^{(alg1)}$ or $\text{loss}_2^{(alg2)}$ w.r.t. $\mathbf{W}^{(new2)}$ and set this gradient to be 0:

$$\mathbf{W}^{(new2)} = (\mathbf{A}^{(new)\top} \mathbf{A}^{(new)})^{-1} \mathbf{A}^{(new)\top} \mathbf{O}^{(2)'}. \quad (11)$$

3 Experiment

We empirically compare CompNet with NetMorph [28] on MNIST and CIFAR10 dataset. We apply our algorithms in three neural network structures, namely LeNet, VGG16 (VGG D with 16 layers) and VGG19 (VGG E with 19 layers) [18, 26] respectively. LeNet with 4 layers is denoted as LeNet4.

In all experiments, we morph the well trained neural network with an additional layer which contains potentially redundant neurons or channels. We denote the neuron size before the sparse optimization as $N_{\text{redundant}}$. Then, we use the same neuron size $N_{\text{redundant}}$ in NetMorph to compare, termed as *NetMorph-Redundant*. And in addition, we equip NetMorph with an unfair advantage to manually set the number of neurons to be N_{sparse} which is the neuron size after sparse optimization in Algorithm 2 to compare. We term this NetMorph setting to be *NetMorph-Oracle*.

3.1 Parameter setting up

For MNIST, we morph from LeNet4 to LetNet5 by adding a convolutional layer. MNIST of handwritten digits includes a training set of 60,000 examples, and a test set of 10,000 examples that are used as training dataset and validation dataset respectively. We use $5e-3$ and $1e-6$ as learning rate and weight decay respectively in LeNet experiments. For CIFAR10, we morph from VGG15 to VGG16, from VGG16 to VGG17 and from VGG18 to VGG19 by adding one convolutional layer respectively. It is popular to insert batch normalization layers to VGG models. However, we don't use batch normalization for simplicity and it can be easily extended to the batch normalization setting for our algorithms. We use $3e-4$ and $1e-6$ as the learning rate and weight decay respectively in VGG experiments. CIFAR10 contains 50,000 training images and 10,000 test images that are used as training dataset and validation dataset respectively. We also use some common techniques to prevent over-fitting such as dropout, l_2 regularizer and data augmentation. For the optimization method, we use SGD with momentum value of 0.9. And we set the λ and α in iiLasso to be 0.1 to test.

3.2 LeNet4 to LeNet5

We train LeNet4 for 200 epochs on MNIST dataset as the parent neural network to morph. And then we insert one convolutional layer with 100 filters and ReLU

activation function between the two convolutional layers of LeNet4, denoted as LetNet5. The result is shown in Figure 2a and Table 2. We can see that CompNet Alg1 gets 99.15% accuracy on epoch 25, CompNet Alg2 gets 99.19% accuracy on epoch 19, CompNet Alg3 gets 99.17% accuracy on epoch 92, NetMorph-Oracle gets 99.17% on epoch 88 and NetMorph-Redundant gets 99.18% on epoch 89 and Scratch gets 99.19% on epoch 84. Our algorithms and NetMorph can converge fast. But in this case, CompNet Alg2 converges fastest and gets best accuracy rate. And Table 1 shows the N_{sparse} and the average compression ratio for our three algorithms.

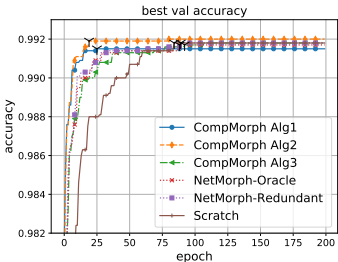
	N_redundant	Alg1	Alg2	Alg3	Avg compress rate
LeNet4 to LeNet5 (ReLU)	100	41	46	49	45.3%
VGG15 to VGG16 (ReLU)	512	165	200	255	40.4%
VGG15 to VGG16 (Sigmoid)	512	196	162	105	30.1%
VGG15 to VGG16 (TanH)	512	213	178	157	35.7%
VGG16 to VGG17 (ReLU)	256	155	121	127	52.5%
VGG18 to VGG19 (ReLU)	512	221	211	255	44.5%

Table 1: Number of neurons before and after sparsifying for each algorithm.

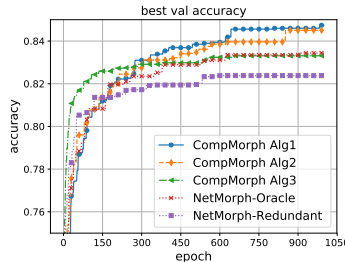
	Alg1	Alg2	Alg3	NetMorph-Oracle	NetMorph-Redundant	Scratch
LeNet4 to LeNet5 (ReLU)	99.15%	99.20%	99.18%	99.17%	99.18%	99.19%
VGG15 to VGG16 (ReLU)	84.74%	84.50%	83.31%	83.44 %	82.38%	83.14%
VGG15 to VGG16 (Sigmoid)	83.63%	83.71%	83.08%	83.25%	82.54%	69.97%
VGG15 to VGG16 (TanH)	83.68%	83.52%	83.86%	83.41%	83.00%	80.70%
VGG16 to VGG17 (ReLU)	85.45%	85.37%	85.78%	85.69%	85.51%	82.71%
VGG18 to VGG19 (ReLU)	89.00%	88.84%	88.90%	88.95%	88.87%	85.26%

Table 2: Best validation accuracy in different experiments.

3.3 VGG15 to VGG16



(a) LetNet4 to LeNet5



(b) VGG15 to VGG16

Figure 2: Left: LetNet4 to LeNet5 with ReLU activation function. Right: VGG15 to VGG16 with ReLU activation function.

It can be seen that Algorithm 3 converges fastest, and Algorithm 1 and 2 are much better than NetMorph-Redundant and NetMorph-Oracle. We also notice that NetMorph-Oracle converges similar to NetMorph-Redundant, but NetMorph-Oracle gets better accuracy which means that the *redundant neurons or channels sparsified by CompNet is really working*. Table 2 shows the best validation accuracy for different algorithms in this setting and Algorithm 1 works best. Finally, we also train the new model VGG16 from scratch for 2,000 epochs. And best validation accuracy for this case is about 83.14% which is worse than our algorithms that are better than 84.00% and only trained for 1,000 epochs in the same setting. We do not draw the validation curve for scratch in this experiment and the following experiments, because the scratch method converges very slow and the

We firstly remove the first convolutional layer with 512 filters and ReLU activation function from VGG16, denoted as VGG15. Afterwards, we train VGG15 from scratch for enough long time, i.e., 1,000 epochs, until its validation accuracy converges. Then we insert the removed convolutional layer back with the initial 512 filters and ReLU activation function to VGG15. The results are shown in Figure 2b.

scale of the figure usually ranges from 40% to 90% in the vertical axis so that we cannot see the other curves clearly.

Moreover, we also insert a convolutional layer with Sigmoid and TanH activation function and the results are shown in Figure 3. In both cases, we can see that Algorithm 1 and 2 get better validation accuracy than NetMorph-Redundant and NetMorph-Oracle. Meanwhile, the validation accuracies training from scratch for TanH and Sigmoid networks with same epochs are 80.70% and 69.97% respectively, which are both worse than CompNet and NetMorph especially for the Sigmoid network. This is potentially because Sigmoid with value in range $[0,1]$ is easier to encounter the saturation problem than TanH with value in range $[-1,1]$.

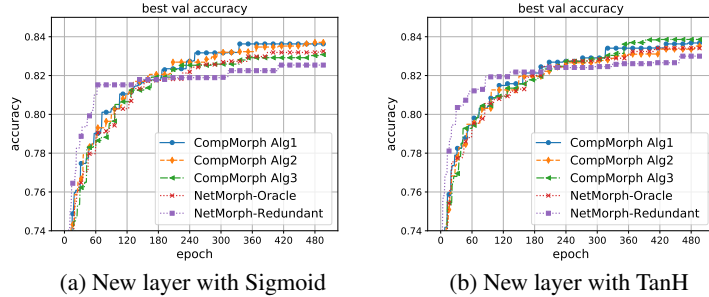


Figure 3: Adding one new layer with Sigmoid and TanH activation function respectively from VGG15 to VGG16.

3.4 VGG16 to VGG17

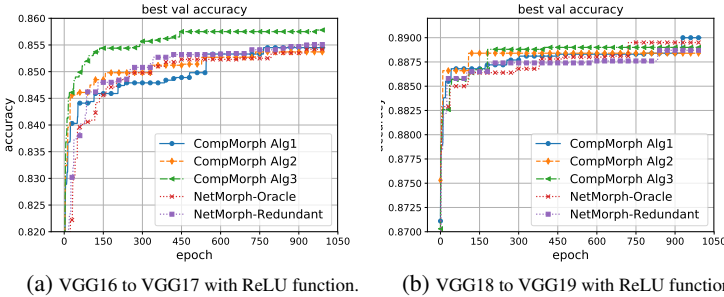


Figure 4: Left: VGG16 to VGG17 with ReLU activation function. Right: VGG18 to VGG19 with ReLU activation function.

ing gradient [11] and singularities [22]. Our algorithms and NetMorph seem to alleviate the two problems according to our results where the best accuracies are higher than 85% in the same setting as shown in Figure 4a. Algorithm 1 and 2 get similar result as NetMorph-Redundant and NetMorph-Oracle but Algorithm 3 gets best accuracy. Table 2 summarizes the best accuracy for different algorithms.

3.5 VGG18 to VGG19

Similarly, we firstly remove one convolutional layer with 512 filters and ReLU activation function from VGG19 denoted as VGG18. We train VGG18 until convergence and then add the removed convolutional layer back with our algorithms. Figure 4b shows the performance of different algorithms. We can see that all the algorithms converge similarly but Algorithm 1 gets best accuracy. The best validation accuracies for different algorithms is summarized in Table 2. We also train VGG19 from scratch for 2,000 epochs and it only gets the best accuracy of 85.26% which is much worse than the accuracy of our algorithms.

We choose the well tuned model of VGG16 with ReLU activation function from the Section 3.3 and continue to insert one convolutional layer with 256 filters and ReLU activation to the selected model, denoted as VGG17. We also train VGG17 model from scratch for 2,000 epochs and its best accuracy is **82.71%** which is much lower than the best accuracy **83.14%** of VGG16 trained from scratch. It may be caused by vanishing

References

- [1] Dzmitry Bahdanau, Kyunghyun Cho, and Yoshua Bengio. Neural machine translation by jointly learning to align and translate. *arXiv preprint arXiv:1409.0473*, 2014.
- [2] Irwan Bello, Barret Zoph, Vijay Vasudevan, and Quoc V Le. Neural optimizer search with reinforcement learning. *arXiv preprint arXiv:1709.07417*, 2017.
- [3] Evgeny Burnaev, Ivan Koptelov, German Novikov, and Timur Khanipov. Automatic construction of a recurrent neural network based classifier for vehicle passage detection. In *Ninth International Conference on Machine Vision (ICMV 2016)*, volume 10341, pp. 1034103. International Society for Optics and Photonics, 2017.
- [4] Tianqi Chen, Ian Goodfellow, and Jonathon Shlens. Net2net: Accelerating learning via knowledge transfer. *arXiv preprint arXiv:1511.05641*, 2015.
- [5] Yu Cheng, Duo Wang, Pan Zhou, and Tao Zhang. A Survey of Model Compression and Acceleration for Deep Neural Networks. *arXiv preprint arXiv:1710.09282*, 2017.
- [6] Kyunghyun Cho, Bart Van Merriënboer, Dzmitry Bahdanau, and Yoshua Bengio. On the properties of neural machine translation: Encoder-decoder approaches. *arXiv preprint arXiv:1409.1259*, 2014.
- [7] Dan Ciregan, Ueli Meier, and Jürgen Schmidhuber. Multi-column deep neural networks for image classification. In *Computer Vision and Pattern Recognition (CVPR), 2012 IEEE Conference on*, pp. 3642–3649. IEEE, 2012.
- [8] Ray J Frank, Neil Davey, and Stephen P Hunt. Time series prediction and neural networks. *Journal of Intelligent & Robotic Systems*, 31(1):91–103, 2001.
- [9] Yarín Gal. *Uncertainty in deep learning*. PhD thesis, PhD thesis, University of Cambridge, 2016.
- [10] Kaiming He, Xiangyu Zhang, Shaoqing Ren, and Jian Sun. Delving deep into rectifiers: Surpassing human-level performance on imagenet classification. In *Proceedings of the IEEE international conference on computer vision*, pp. 1026–1034, 2015.
- [11] Kaiming He, Xiangyu Zhang, Shaoqing Ren, and Jian Sun. Deep residual learning for image recognition. In *Proceedings of the IEEE conference on computer vision and pattern recognition*, pp. 770–778, 2016.
- [12] Yihui He, Xiangyu Zhang, and Jian Sun. Channel pruning for accelerating very deep neural networks. In *International Conference on Computer Vision (ICCV)*, volume 2, pp. 6, 2017.
- [13] Geoffrey Hinton, Oriol Vinyals, and Jeff Dean. Distilling the knowledge in a neural network. *arXiv preprint arXiv:1503.02531*, 2015.
- [14] Nal Kalchbrenner and Phil Blunsom. Recurrent continuous translation models. In *EMNLP*, volume 3, pp. 413, 2013.
- [15] Kyoung-jae Kim. Artificial neural networks with evolutionary instance selection for financial forecasting. *Expert Systems with Applications*, 30(3):519–526, 2006.
- [16] Alex Krizhevsky, Ilya Sutskever, and Geoffrey E Hinton. Imagenet classification with deep convolutional neural networks. In *Advances in neural information processing systems*, pp. 1097–1105, 2012.
- [17] Siddharth Krishna Kumar. On weight initialization in deep neural networks. *arXiv preprint arXiv:1704.08863*, 2017.
- [18] Yann LeCun et al. Lenet-5, convolutional neural networks.
- [19] Jun Lu. Machine learning modeling for time series problem: Predicting flight ticket prices. *arXiv preprint arXiv:1705.07205*, 2017.
- [20] Wei Ma and Jun Lu. An Equivalence of Fully Connected Layer and Convolutional Layer. *arXiv preprint arXiv:1712.01252*, 2017.
- [21] R Muthukrishnan and R Rohini. Lasso: A feature selection technique in predictive modeling for machine learning. In *Advances in Computer Applications (ICACA), IEEE International Conference on*, pp. 18–20. IEEE, 2016.
- [22] A Emin Orhan. Skip connections as effective symmetry-breaking. *arXiv preprint arXiv:1701.09175*, 2017.
- [23] Prajit Ramachandran, Barret Zoph, and Quoc Le. Searching for activation functions. 2017.
- [24] Shaoqing Ren, Kaiming He, Ross Girshick, and Jian Sun. Faster r-cnn: Towards real-time object detection with region proposal networks. In *Advances in neural information processing systems*, pp. 91–99, 2015.
- [25] Henry A Rowley, Shumeet Baluja, and Takeo Kanade. Neural network-based face detection. *IEEE Transactions on pattern analysis and machine intelligence*, 20(1):23–38, 1998.
- [26] Karen Simonyan and Andrew Zisserman. Very deep convolutional networks for large-scale image recognition. *arXiv preprint arXiv:1409.1556*, 2014.
- [27] M. Takada, T. Suzuki, and H. Fujisawa. Independently Interpretable Lasso: A New Regularizer for Sparse Regression with Uncorrelated Variables. *ArXiv e-prints*, November 2017.
- [28] Tao Wei, Changhu Wang, Yong Rui, and Chang Wen Chen. Network morphism. In *International Conference on Machine Learning*, pp. 564–572, 2016.